Power System State Estimation Using Three-Phase Models

C. W. Hansen, Member, IEEE A. S. Debs, Senior Member, IEEE

Decision Systems International
Atlanta, Georgia USA

Abstract **– Phase imbalances can occur at both the distribution and transmission levels of an electric power system. It is shown that these imbalances can have a significant negative impact upon the performance of a state estimator which utilizes only a positive-sequence model of the power system. A state estimator which uses a full three-phase model of the system is developed and various transmission and distribution networks are simulated. Depending on the level of imbalances, the improvement in state estimator accuracy can be dramatic. In addition, a plausible explanation for large reactive power measurement errors is presented and empirically validated.**

I. INTRODUCTION

A simplifying assumption made in most power system calculations is that the system is balanced. This means that, except for a 120-degree phase shift, all three phases have the same voltage, current, and power flow profiles. This assumption is extremely powerful since the three-phase system can be reduced to the much simpler positive-sequence system.

In practice, unbalanced conditions can occur in both the system loads and in the network itself. Load imbalances are most pronounced at the distribution level. These imbalances are caused by uneven single-phase loads. Network model imbalances occur mainly at the transmission level of the system. These imbalances arise from untransposed transmission lines and from multiple lines sharing one physical right-of-way. Thus, a strong case can be made against the standard assumption that positive-sequence models are always acceptable in state estimation.

A state estimator which determines the full three-phase system state would have at least two significant benefits. First, since the model is more accurate, the state estimate will contain less systematic errors. Secondly, the real-time monitoring of all three phases will allow the detection of phase imbalances. This could identify potential problems such as machine overheating and improper relay operation. In addition, information about system losses could be quantified and then used to improve economic performance.

94 SM 601-5 PWRS A paper recommended and approved by the IEEE Power System Engineering Committee of the IEEE Power Engineering Society for presentation at the IEEE/PES 1994 Summer Meeting, San Francisco, CA, July 24-28, 1994. Manuscript submitted December 23, 1993; made available for printing June 2, 1994.

II. IMBALANCES IN A THREE-PHASE MODEL

A typical high-voltage transmission line is shown in Fig. 1 [2]. Two electrically separate lines are placed on the same tower, perhaps for economic reasons. Each line has two conductors per phase and there are two ground wires located at the top of the tower.

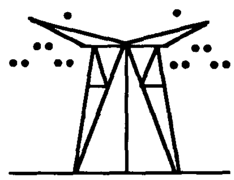

Fig 1. Transmission Tower Configuration

The series impedance matrix for this double-circuit transmission line is shown in Fig. 2.

$$Z_S = \begin{array}{c} 1(X) \\ 1(Y) \\ 1(Z) \\ 2(X) \\ 2(Y) \\ 2(Z) \end{array} \left[\begin{array}{ccc|ccc} .19+j1.10 & & & & & \\ .13+j.52 & .20+j1.09 & & & & \\ .12+j.54 & .13+j.51 & .19+j1.10 & & & \\ \hline .13+j.53 & .13+j.46 & .12+j.45 & .19+j1.10 & & \\ .13+j.46 & .13+j.45 & .13+j.42 & .13+j.52 & .20+j1.09 & \\ .12+j.45 & .13+j.42 & .12+j.41 & .12+j.54 & .13+j.51 & .19+j1.10 \end{array}\right]$$

Fig. 2. Series Impedance Matrix

Notice that several characteristics of this line would be ignored by the standard positive-sequence model. The diagonal elements are not identical to each other. The coupling between the lines (lower-left) is significant because the current flowing through Line 1 has a meaningful impact upon the current flowing in Line 2. Also, note that even the coupling between the phases of a given line is not symmetrical.

Of course there are techniques which can be used to lessen these network imbalances. The phases of a particular line can be transposed at regular intervals. It is also conceivable to transpose entire lines to help reduce the effects of unbalanced coupling. It is still possible, however, that significant imbalances may remain. Transposition may not be implemented perfectly. Also, transmission line corridors are becoming increasingly crowded due to the difficulty of obtaining new right-of-ways. Thus, it is often the case that several transmission lines, perhaps even of different voltage levels, will share a given corridor. Since the standard state estimator model cannot consider such coupling, large estimate errors will occur.

At the distribution level, even larger imbalances can be observed. Commercial and residential loads require single-phase transformers. Utilities will attempt to distribute these single-phase loads equally amongst the three phases, but inevitably, significant imbalances will occur. Table 1 shows actual phase currents obtained from an industrial power distribution system.

TABLE 1. PHASE CURRENTS FROM A DISTRIBUTION SYSTEM

Phase Currents (Amps)			Maximum
X	Y	Z	Difference
224	261	253	14%
105	118	113	11%
397	406	418	5%
150	168	152	11%
452	460	473	4%
123	128	106	17%
102	117	113	13%
213	219	201	8%

If a transformer has an ungrounded winding connection (i.e. ungrounded-wye or delta) and is then subjected to unbalanced power flows, the phases will no longer be independent from each other. In other words, the standard state estimator model will introduce additional errors into the state estimate.

III. THREE-PHASE WLS STATE ESTIMATION

The three-phase weighted-least-squares state estimator can be formulated as follows. Suppose a network consists of a total of N_b buses, N_g of which are generator buses. There are six states for each bus, consisting of voltage magnitudes (V_a, V_b, V_c) and phase angles $(\delta_a, \delta_b, \delta_c)$. For each generator bus, there is an associated internal bus with balanced excitation which is the same model proposed for the three-phase load flow problem [3-6]. Each of these internal buses has two states $(V_{\text{int}}, \delta_{\text{int}})$, except for the slack bus. As in the standard case, the slack bus has only one state (V_{slack}) because $\delta_{slack} \equiv 0$. Thus, the state vector, $\mathbf{x}$, is an $n \times 1$ vector, where $n = 6N_b + 2N_g - 1$. Let the $m \times 1$ vector of measurements, $\mathbf{z}$, be described as a function of the state vector, plus an error vector, υ:

$$\mathbf{z} = \mathbf{h}(\mathbf{x}) + \upsilon, \text{ where } E\{\upsilon\} = \mathbf{0} \text{ and } E\{\upsilon\upsilon^T\} = \mathbf{R} \tag{1}$$

The measurement vector, $\mathbf{z}$, typically includes voltage magnitudes, active power (Watts), and reactive power (Vars). Power flow equations are used to describe power flow/injection measurements in terms of the system state ($\mathbf{x}$). When using the standard single-phase model, the power injected at bus k is:

$$\begin{aligned} P_i &= V_i \sum_{k=1}^{n} V_k \left[G_{ik}\cos(\theta_{ik}) + B_{ik}\sin(\theta_{ik})\right] \\ Q_i &= V_i \sum_{k=1}^{n} V_k \left[G_{ik}\sin(\theta_{ik}) - B_{ik}\cos(\theta_{ik})\right] \end{aligned} \tag{2}$$

The significant difference between single-phase and three-phase power flows is that all three phases impact the power flowing in any one phase. Thus, for a three-phase model, the power injected at bus k in phase p can be written as:

$$\begin{aligned} P_i^p &= V_i^p \sum_{k=1}^{n}\sum_{m=1}^{3} V_k^m \left[G_{ik}^{pm}\cos(\theta_{ik}^{pm}) + B_{ki}^{pm}\sin(\theta_{ik}^{pm})\right] \\ Q_i^p &= V_i^p \sum_{k=1}^{n}\sum_{m=1}^{3} V_k^m \left[G_{ik}^{pm}\sin(\theta_{ik}^{pm}) - B_{ik}^{pm}\cos(\theta_{ik}^{pm})\right] \end{aligned} \tag{3}$$

where $Y = G + jB$ is the system admittance matrix

The construction of the three-phase admittance matrix is discussed in Appendix A.

In addition to telemetered measurements, which are subject to error, there are "perfect" measurements. At buses with no loads, it is known that the net power injected into the bus from the network is zero. These *zero-injection* measurements can be included into the state estimator as a set of equality constraints, $\mathbf{c}(\mathbf{x}) = \mathbf{0}$.

The weighted-least-squares optimization takes on the following form:

$$\begin{aligned} &\textit{Minimize } J(\mathbf{x}) = [\mathbf{z} - \mathbf{h}(\mathbf{x})]^T \mathbf{R}^{-1} [\mathbf{z} - \mathbf{h}(\mathbf{x})] \\ &\quad \textit{such that } \mathbf{c}(\mathbf{x}) = \mathbf{0} \end{aligned} \tag{4}$$

The Lagrangian is formed as:

$$L(\mathbf{x}, \lambda) = \frac{1}{2}[\mathbf{z} - \mathbf{h}(\mathbf{x})]^T \mathbf{R}^{-1}[\mathbf{z} - \mathbf{h}(\mathbf{x})] + \lambda^T \mathbf{c}(\mathbf{x}) \tag{5}$$

Minimizing the Lagrangian is accomplished by setting the partial derivatives with respect to $\mathbf{x}$ and λ to zero:

$$\mathbf{0} = \mathbf{f}(\mathbf{x}) \equiv \frac{\partial L(\mathbf{x}, \lambda)}{\partial \mathbf{x}} \Rightarrow \mathbf{H}^T \mathbf{R}^{-1}[\mathbf{z} - \mathbf{h}(\mathbf{x})] - \mathbf{C}^T \lambda = \mathbf{0} \tag{6a}$$

$$\mathbf{0} = \frac{\partial L(\mathbf{x}, \lambda)}{\partial \lambda} \Rightarrow \mathbf{c}(\mathbf{x}) = \mathbf{0} \tag{6b}$$

$\mathbf{H}(\mathbf{x})$ is the telemetered-measurement Jacobian matrix and $\mathbf{C}(\mathbf{x})$ is the Jacobian matrix corresponding to the zero-injections. Since $\mathbf{h}(\bullet)$ and $\mathbf{c}(\bullet)$ are nonlinear set of equations, (6) cannot be solved directly. An iterative approach, such as Newton's Method, needs to be used:

$$\begin{bmatrix} \frac{\partial \mathbf{f}}{\partial x} & \frac{\partial \mathbf{f}}{\partial \lambda} \\ \frac{\partial \mathbf{c}}{\partial x} & \frac{\partial \mathbf{c}}{\partial \lambda} \end{bmatrix} \begin{bmatrix} \Delta \mathbf{x} \\ \Delta \lambda \end{bmatrix} = \begin{bmatrix} -\mathbf{f}(\mathbf{x}_k, \lambda_k) \\ -\mathbf{c}(\mathbf{x}_k, \lambda_k) \end{bmatrix} \tag{7}$$

$$\text{where } \mathbf{x}_{k+1} = \mathbf{x}_k + \Delta \mathbf{x} \text{ and } \lambda_{k+1} = \lambda_k + \Delta \lambda$$

Rewriting $\mathbf{f}(\mathbf{x})$ and taking the partial derivatives gives:

$$\mathbf{f}(\mathbf{x}) = \sum_{i=1}^{m} \frac{\partial h_i(\mathbf{x})}{\partial \mathbf{x}} \frac{z_i - h_i(\mathbf{x})}{\sigma_i^2} - \sum_{j=1}^{nc} \lambda_j \frac{\partial c_j(\mathbf{x})}{\partial \mathbf{x}} \tag{8a}$$

$$\frac{\partial \mathbf{f}}{\partial \mathbf{x}} = -\sum_{i=1}^{m} \frac{1}{\sigma_i^2} \frac{\partial h_i}{\partial \mathbf{x}} \left(\frac{\partial h_i}{\partial \mathbf{x}} \right)^T = -\mathbf{H}^T \mathbf{R}^{-1} \mathbf{H} \tag{8b}$$

$$\frac{\partial \mathbf{f}}{\partial \lambda} = -\sum_{j=1}^{nc} \frac{\partial c_j}{\partial \mathbf{x}} = -\mathbf{C}^T \tag{8c}$$

Combining and simplifying the above relations yields,

$$\begin{bmatrix} \mathbf{H}^T \mathbf{R}^{-1} \mathbf{H} & \mathbf{C}^T \\ \mathbf{C} & \mathbf{0} \end{bmatrix} \begin{bmatrix} \Delta \mathbf{x} \\ \lambda_{k+1} \end{bmatrix} = \begin{bmatrix} H^T R^{-1}(\mathbf{z} - \mathbf{h}(\mathbf{x}_k)) \\ -\mathbf{c}(\mathbf{x}_k) \end{bmatrix} \tag{9}$$

Newton's Method requires the repeated calculations of $\Delta \mathbf{x}$. The iterative process continues until $\Delta \mathbf{x}$ becomes very small, and the resulting value of $\mathbf{x}_k$ is called the state estimate $(\hat{\mathbf{x}})$.

This formulation (9) is called the *equality constraint* formulation. Another formulation is *Hachtel's Augmented Matrix* [8]. Define the measurement and residual errors as:

$$\begin{aligned} \Delta \mathbf{z} &= \mathbf{z} - \mathbf{h}(\mathbf{x}_k) \\ \Delta \mathbf{r} &= \Delta \mathbf{z} - \mathbf{H} \Delta \mathbf{x} \end{aligned} \tag{10}$$

Hachtel's formulation can then be expressed as:

$$\begin{bmatrix} \mathbf{R} & \mathbf{H} & \mathbf{0} \\ \mathbf{H}^T & \mathbf{0} & \mathbf{C}^T \\ \mathbf{0} & \mathbf{C} & \mathbf{0} \end{bmatrix} \begin{bmatrix} \mathbf{R}^{-1} \Delta \mathbf{r} \\ \Delta \mathbf{x} \\ -\lambda_{k+1} \end{bmatrix} = \begin{bmatrix} \Delta \mathbf{z} \\ \mathbf{0} \\ -\mathbf{c}(\mathbf{x}_k) \end{bmatrix} \tag{11}$$

IV. Testing Method

In order to quantify the relative performance of the three-phase and positive-sequence state estimators, the testing method shown in Fig. 3 was employed.

The 3-Ø Load Flow simulates the network, including any load and/or model imbalances. The Measurement Maker then computes true and noisy values for the specified measurements. Measurements for all three-phases are given to the 3-Ø Estimator. Since the positive-sequence (1-Ø) estimator cannot handle 3-Ø information directly, three state estimates must be calculated (one for each phase). The results of these three runs are combined and compared to the single 3-Ø estimate.

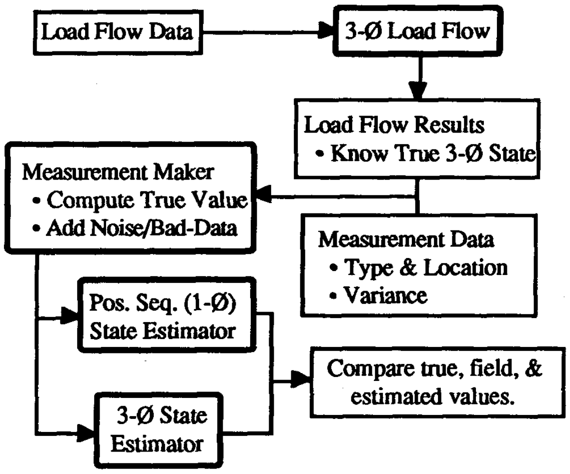

Fig. 3. Testing Method for 3-Ø Estimator

A method to compare the relative accuracy of the single-phase and three-phase state estimates is required. The first performance index is simply the optimality function which is being minimized. That is:

$$J = \sum_{i=1}^{m} \frac{\left(z_i^{measured} - z_i^{estimated} \right)^2}{\sigma_i^2} \tag{12}$$

This number is useful because the better a given model fits the data, the lower the performance index will become. A better gauge for estimate accuracy, however, is the proximity of the estimated measurements to their true values. That is:

$$J_{true} = \sum_{i=1}^{m} \frac{\left(z_i^{true} - z_i^{estimated} \right)^2}{\sigma_i^2} \tag{13}$$

Notice that this performance index can't be computed for actual system data since the true measurements are not known.

V. Results

Results from a transmission network and a distribution network are presented. The first network (Fig. 4) simulates a portion of a high-voltage transmission system [6]. There are two generator buses and four load buses. Four zero-injection buses have been created to handle the change in line coupling. The network contains two delta:grounded-wye transformers, two single-circuit transmission lines, two double-circuit transmission lines, and one quadruple-circuit transmission line.

Eight separate cases are run for this network. The loads can be either balanced or unbalanced. The transmission line parameters can either balanced or unbalanced. Also, the measurement simulator can either make perfect measurements (no noise) or it can simulate a real system by adding measurement noise.

Note that all imbalances have been limited to 5%, which is conservative in light of the discussion in Section 2.

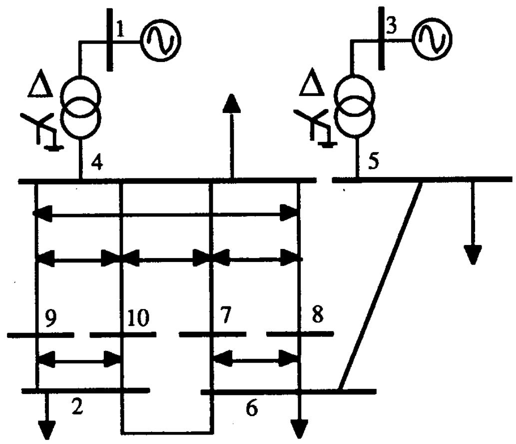

Fig. 4. Transmission network with line-coupling

The results for all eight cases are shown in Table 2. In the first two cases, the load and model are balanced. As expected, the single-phase and three-phase estimators perform identically.

In the third and fourth cases, the model for the system is imbalanced, so the positive-sequence model is no longer adequate. Even when the measurements are perfect (case 3), the single-phase estimator is no longer able to obtain the proper estimates (J = 27). When measurement noise is added (case 4), J_{true} for the three-phase estimate is 48% smaller than for the combined single-phase estimates.

TABLE 2 PERFORMANCE FOR TRANSMISSION SYSTEM

	Load Bal?	Network Bal?	Perfect msmt	1-Ø Estimate J	1-Ø Estimate J_{true}	3-Ø Estimate J	3-Ø Estimate J_{true}	Improvement (%) J	Improvement (%) J_{true}
1	yes	yes	yes	0	0	0	0	–	–
2	yes	yes	no	132	23	132	23	–	–
3	yes	no	yes	27	27	0	0	100	100
4	yes	no	no	120	66	99	34	18	48
5	no	yes	yes	29	29	0	0	100	100
6	no	yes	no	132	51	106	21	20	60
7	no	no	yes	53	53	0	0	100	100
8	no	no	no	170	83	111	37	35	55

In cases five and six, the model is balanced while the loads are unbalanced. Once again, even when the single-phase estimator is given exact measurements (case 5), it cannot come up with the proper measurement values. In case 6, measurement noise is added. J_{true} for the three-phase estimator is 60% smaller than for the single-phase estimator.

Finally, both the network and load are allowed to be unbalanced. Notice that this combination makes the single-phase estimator performance degrade even further. As before, even when the single-phase state estimator is given perfect measurements, large errors result. When realistic measurement noise is added, the three-phase state estimator shows a significant 55% decrease in the J_{true} performance index.

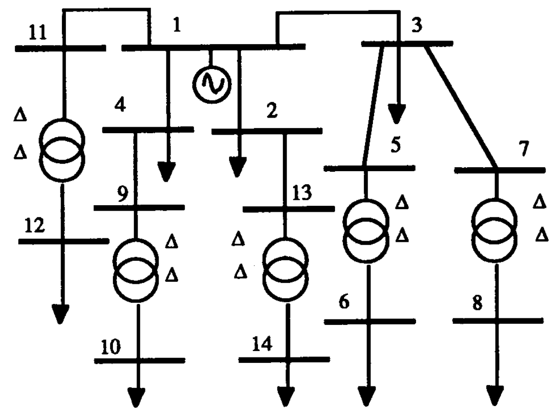

Fig. 5. Industrial Distribution Network

The next network (Fig. 5) simulates a portion of an actual industrial distribution network. This network is a radial system with five delta-delta transformers, two of which have off-nominal taps. The unbalanced load pattern is taken from an actual snapshot of the system. To be conservative, the network model is assumed to be balanced and lines are uncoupled. The connection to the local utility is modeled as a generator. There are 183 measurements and 30 zero-injection constraints. This gives the network a measurement to state ratio of 2.5.

The improvement of the three-phase state estimator is just as dramatic for the distribution system as it is for the transmission system (Table 3). In case 9, the estimators are given "perfect" measurements. The three-phase state estimator perfectly estimates the state, while the single-phase estimator, due to the model inadequacies, fails to do so.

TABLE 3. PERFORMANCE FOR DISTRIBUTION SYSTEM

	Load Bal?	Network Bal?	Perfect msmt	1-Ø Estimate J	1-Ø Estimate J_{true}	3-Ø Estimate J	3-Ø Estimate J_{true}	Improvement (%) J	Improvement (%) J_{true}
9	no	yes	yes	36	36	0	0	100	100
10	no	yes	no	168	83	122	42	27	50

Case 10 is more realistic since noise has been added to the measurements. Although the three-phase state estimator can no longer "perfectly" estimate the state, J_{true} has been cut in half.

Since we know the true state in these simulations, a performance index based upon the state can be defined:

$$P_3 = \sqrt{\frac{1}{n}\sum_{i=1}^{n}\left(x_i^{true} - x_i^{estimate}\right)^2} \tag{14}$$

For case 10, P_3 is 46% smaller for voltage magnitude states and 47% smaller for angle states.

VI. CONVERGENCE AND PERFORMANCE

It has been the experience of the authors that the Newton-Raphson formulation of the three-phase state estimator yields quadratic convergence characteristics. In other words, the three-phase estimator requires the same number of iterations to converge as the single-phase estimator.

Of course the computational effort of the three-phase state estimator is much greater. Many loops in the computer code must be tripled. Non-zeros increase in response to the replacement of single elements by 3x1 and 3x3 blocks. In this light, it is reasonable to expect that the overall computational cost of the three-phase state estimator would fall somewhere between three to nine-times that of the single-phase estimator.

This has been observed in actual testing. The execution time was monitored for the distribution network (Fig. 5). Both the three-phase and single-phase estimators began from a flat start and converged in five iterations. The three-phase estimator required 9.212 seconds to solve while the single-phase estimator required 1.533 seconds (Mac IIci computer). This makes the three-phase state estimator 6.01 times slower.

It is important to note that both the single-phase and three-phase state estimators employ sparsity techniques.

VII. REACTIVE POWER MEASUREMENT RESIDUALS

Many on-line state estimators consistently encounter relatively large reactive power (MVar) measurement residual errors as compared to corresponding active power (MW) measurements. This phenomenon has been observed during the testing of the three-phase state estimator.

The following index expresses the error in the state estimate over a set of measurements (1,...,k).

$$E_{avg} = \sqrt{\frac{1}{k}\sum_{i=1}^{k}\left(z_i - h_i(\mathbf{x})\right)^2} \tag{15}$$

This index is now computed for different measurement subsets of Case 2 (Table 3) above. For the three-phase state estimator,

$$E_{avg}^{active\ flows} = 1.8MW \tag{16}$$

$$E_{avg}^{reactive\ flows} = 1.8MVar \tag{17}$$

Notice that the average measurement error is the same for active and reactive measurements. For the combined positive-sequence (1-Ø) estimates,

$$E_{avg}^{active\ flows} = 3.0MW \tag{18}$$

$$E_{avg}^{reactive\ flows} = 4.1MVar \tag{19}$$

As expected, the average error for the single-phase state estimates is higher. In particular, the average error for the MVar measurements has more than doubled. In this case, this discrepancy can be attributed to the delta-delta connected transformers. The equivalent three-phase admittance model for this transformer contains substantial phase-to-phase connections. Since the X/R ratio for a transformer is quite high, the impact of ignoring this information (as the positive-sequence model does) is stronger upon reactive power measurements than upon real power measurements.

VIII. CONSIDERATIONS FOR A PRACTICAL 3-Ø ESTIMATOR

There are many requirements for an on-line state estimator, and a three-phase model has a definite impact upon these demands. Some of the unique requirements for a three-phase on-line state estimator are discussed next. Note that many of these issues are outside the scope of this paper.

A. Observability

The observability routine must decide if the measurement set is sufficient in type and distribution to allow the computation of the state estimate. If the measurement set is deficient, this routine should determine which sub-networks are observable, as well as where additional measurements could be added to make the entire network observable. Observability for a three-phase state estimator is similar to the single-phase case, but there are notable differences. These differences arise from the coupling of phases, coupling of parallel-transmission lines, and from new types of measurements.

If all three phases of a system are measured at the exact same points and no coupling exists between any two lines, then three-phase observability reduces to single-phase observability.

Coupling between the phases of a given line, as well as coupling between parallel lines, must be considered by the three-phase observability routine. For instance, the power flowing on an uncoupled line is a function only of the state variables of the two terminal buses. If a line is electrically-coupled to a parallel line, the power flow is now a function of the state variables of *four* buses. Such additional coupling could allow a three-phase system to be observable, even when one of the corresponding individual phases is unobservable.

The coupling between phases or between lines is not as strong as the link between the same-phase of neighboring buses. This could result in a three-phase network being classified as topologically observable, but not solvable by the state estimator. Numerical observability methods, which employ actual matrix factorizations, would ensure that the three-phase state estimator could converge from a flat start.

Another difference between single-phase and three-phase observability is that the latter may have to handle different types of measurements. For example, the total three-phase power flowing at a particular point may be measured. This measurement, which is essentially the sum of three single-phase measurements, must clearly be handled differently than a single-phase measurement.

B. Network Configuration

The network configuration routine monitors the positions of system components and determines the system model to be used by the state estimator. Breaker positions, switch positions, and transformer taps are examples of real-time inputs used by the network configurator.

A three-phase model requires additional decisions to be made by this routine. For example, if a line is taken out of commission for maintenance, and this line is coupled to two other parallel lines, the model will have to be adjusted accordingly. Specifically, the admittance matrices associated with these lines will become 6x6, rather than 9x9.

C. Faulty data/parameter detection

Additional complications can arise in the area of measurement and parameter errors. Bad measurements could result when a state estimator is given measurements from incorrect phases. For instance, corresponding x-phase and y-phase measurements may be inadvertently interchanged. If the phases are relatively balanced, this could be troublesome to detect.

Parameters for different phases could similarly be confused. Transmission line models for untransposed and/or mutually-coupled parallel lines, have parameters which vary for each phase. Care must be taken to ensure that the state estimator receives the correct parameters for each of the three phases.

D. Measurement Availability

At the present, it is unlikely that a utility will have complete measurements available for all three-phases. This may change in the near future, however, with the advent of computer relaying. Since all three-phases would be digitally monitored for protection purposes, this information could be easily shared with the SCADA system.

In addition to the standard single-phase power flow measurements, a three-phase state estimator can utilize a variety of measurements. Such new measurements include:

- Total three-phase power
- Sequence-component power and voltage
- Phase-to-phase voltage magnitude
- Voltage phase-angle difference between phases

Since these measurements can be expressed in terms of the state variables, adding them to the three-phase state estimator would be a straight-forward task. The more challenging issue is the impact upon observability, which was discussed earlier.

IX. Conclusion

Imbalances can occur at both the transmission and distribution levels of the power network. It has been demonstrated through simulations that a three-phase model, when implemented into the standard WLS estimator, can yield meaningful improvements in estimator accuracy. These results apply to both distribution and high-voltage transmission networks.

In addition, it is reasonable to believe that these performance gains will be just as significant for other state estimator formulations. All state estimator algorithms rely upon a measurement model, so the WLAV or LMS estimators should also consider the addition of a full three-phase model.

The benefits from a state estimator utilizing a full three-phase state model can be summarized as follows:

- Improved estimates allow better understanding of current operating point
- Three-phase information allows the detection of dangerous imbalances
- Bad-data rejection will improve due to less systematic-modeling errors
- Can determine losses due to system imbalances
- Can study the phenomenon of large reactive power measurement variances

We recommend that further research be conducted in this area. Performance gains need to be validated using actual large-scale system models and measurements. This should be done for both transmission and distribution systems. In addition, observability and bad-data routines must be extended to address the additional requirements of three-phase models. Since this improved modeling requires additional computational effort, optimization of computer code and methods is needed to make on-line state estimation feasible.

X. Acknowledgments

The authors would like to acknowledge the Michigan Division of the Dow Chemical Company for their generous support of this research. Special recognition needs to be given to David Camp, Walt Selle and Chris Schepperly.

This research was largely conducted at the Georgia Institute of Technology, where Dr. Hansen was a graduate student and Dr. Debs was a full professor.

XI. Appendix A. Three Phase Models

A. Transmission Lines

The standard Pi-equivalent model for a transmission line is shown in Fig. 6. The admittances are scalars for the single-phase model and 3x3 blocks for the three-phase model. Also, the voltages and currents for the single-phase model are scalar, while they become 3x1 vectors for the three-phase case.

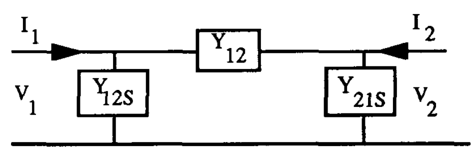

Fig. 6. Pi-equivalent of transmission line

The Pi-equivalent model can even be extended for coupled transmission lines. In general, the dimension of the admittance blocks will be three times the number of parallel transmission lines. For example, consider the coupled lines in Fig. 7.

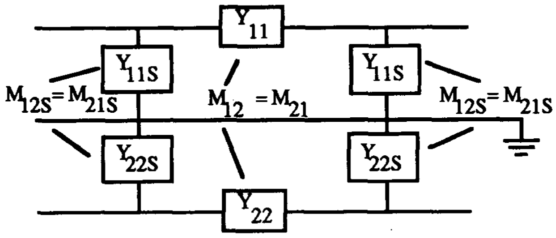

Fig. 7. Coupled transmission lines

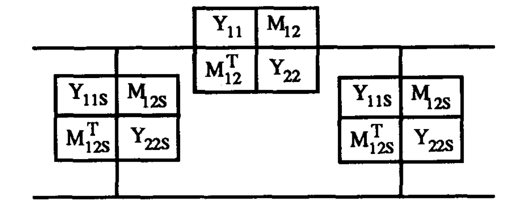

Fig. 8. Equivalent circuit for coupled transmission lines

By creating 6x6 blocks, it is possible to still think of the transmission line in terms of the standard model (Fig. 8).

B. Transformers

Transformers are handled differently in the three-phase case: the winding-connection becomes critically important [2]. Although more complicated than the single-phase case, Table 4 shows how to create admittance matrices for the various transformer connections. Note that Y_t is the leakage reactance.

TABLE 4. THREE-PHASE TRANSFORMER ADMITTANCE MATRIX

Connection	Block A	Block B	Block C
Gnd Y:Gnd Y	I	I	-I
Gnd Y:Y	II	II	-II
Gnd Y:Δ	I	II	III
Y:Y	II	II	-II
Y:Δ	II	II	III
Δ:Δ	II	II	-II

where $Y = \begin{bmatrix} A & C \\ C^T & B \end{bmatrix}$ $\quad I = \begin{bmatrix} Y_t & 0 & 0 \\ 0 & Y_t & 0 \\ 0 & 0 & Y_t \end{bmatrix}$

$$II = \frac{1}{3}\begin{bmatrix} 2Y_t & -Y_t & -Y_t \\ -Y_t & 2Y_t & -Y_t \\ -Y_t & -Y_t & 2Y_t \end{bmatrix} \quad III = \frac{\sqrt{3}}{3}\begin{bmatrix} -Y_t & Y_t & 0 \\ 0 & -Y_t & Y_t \\ Y_t & 0 & -Y_t \end{bmatrix}$$

The effect of tap-changers can be incorporated into the above results. If a is the primary tap ratio (with a = 1.0 being the nominal value), then the admittance matrix becomes:

$$Y = \begin{bmatrix} A/a^2 & C/a \\ C^T/a & B \end{bmatrix} \tag{20}$$

XII. References

[1] F.C. Schweppe and J. Wildes, "Power system static-state estimation, Part I-III," IEEE Trans. on Power App. and Systems, vol. PAS-89, no. 1, January 1970, pp. 120-135.

[2] M. Chen and W. E. Dillon, "Power system modeling", *Proceedings of the IEEE*, vol. 62, no. 7, July 1974, pp. 901-915.

[3] J. Arrillaga and B. J. Harker, "Fast-decoupled three-phase load flow", *Proceedings of the IEEE*, vol. 125, no. 8, August 1978, pp. 734-740.

[4] K. A. Birt, A. H. El-Abiad, J. J. Graffy, and J. D. McDonald, "Three phase load flow program", *IEEE Transactions on Power Apparatus and Systems*, vol. PAS-95, no. 1, January/February 1976, pp.59-65.

[5] R. G. Wasley and M. A. Shlash, "Newton-Raphson algorithm for 3-phase load flow", *Proceedings of the IEEE*, vol. 121, no. 7, July 1974, pp.630-638.

[6] J. Arrillaga, C.P. Arnold, and B.J. Harker, *Computer Modeling of Electrical Power Systems*, John Wiley & Sons, January 1983.

[7] Y. Wallach , *Calculations and Programs For Power System Networks*, Prentice-Hall, Inc., January 1986.

[8] W.H. Liu, F.F. Wu, L. Holten, A. Gjelsvik, and S. Aam, "Computational issues in the Hachtel's augmented matrix method for power system state estimation", *Proceeding of the 9th PSCC*, September 1987, pp. 509-515.

[9] A. S. Debs, *Modern Power Systems Control and Operation*, Kluwer Academic Publishers, Norwell MA, 1988 (Currently available directly from Decision Systems International, Atlanta, GA USA).

[10] C. W. Hansen, *Model Enhancements for State Estimation in Electric Power Systems*, Ph.D. Thesis, Georgia Institute of Technology, December 1993.

[11] M. E. Baran and A. W. Kelley, "State Estimation for real-time monitoring of distribution systems," IEEE/PES 1994 Winter Meeting, New York, Paper 94 WM 235-2 PWRS.

[12] C. N. Lu, J. H. Teng, and W.-H. E. Liu, "Distribution system state estimation," IEEE/PES 1994 Winter Meeting, New York, Paper 94 WM 098-4 PWRS.

XIII. Biographies

Dr. Charles W. Hansen received his Ph.D. in Electrical and Computer Engineering from the Georgia Institute of Technology in December, 1993. His thesis was entitled "Model Enhancements for State Estimation in Electric Power Systems." His research addressed several limitations of on-line state estimators. Specifically, a) the effects of imbalances in the loads and the network on state estimator performance, b) proper modeling of the measurement system to attain an improved estimate, and c) numerical techniques to overcome ill-conditioning problems. Dr. Hansen was a Presidential Fellow and a Dow Fellow while studying at Georgia Tech. He received his Bachelor Degrees in Electrical Engineering and Mathematics from the University of Wisconsin in 1988. Dr. Hansen presently holds the position of Senior Engineer at Decision Systems International.

Dr. Atif S. Debs is President of Decision Systems International and was a Professor of Electrical and Computer Engineering at the Georgia Institute of Technology (Georgia Tech). He was co-founder of Georgia Tech's renowned electric power program at the research and educational levels, which was initiated in 1972. Dr. Debs is a leading expert on control center advanced application functions and system planning. He is the author of *Modern Power Systems Control and Operation*, a large number of technical papers and reports on state estimation, external equivalents, security assessment, dynamic security assessment, production costing, transmission planning, neural networks, and others. He is in the process of completing a book entitled, *Modern Power System Planning*.